Published in the Proceedings of the 16th International Aluminum Alloys Conference (ICAA16) 2018
ISBN: 978-1-926872-41-4
by the Canadian Institute of Mining, Metallurgy & Petroleum

PRECIPITATION KINETICS OF AN AlSi7Cu3.5Mg0.1 ALLOY WITH Zr AND V ADDITIONS

Pierre Heugue[1], *Daniel Larouche[1], Francis Breton[2], Rémi Martinez[3], and X.-Grant Chen[4]

[1] *Laval University, Department of Mining, Metallurgy and Materials Engineering, Aluminum Research Center – REGAL, 1065, ave de la Médecine, Québec, Canada, G1V 0A6*

[2] *Rio Tinto, Arvida Research and Development Centre, 1955, Mellon Blvd, Saguenay, Québec, Canada, G7S 4K8*

[3] *Montupet S.A., 3, rue de Nogent, Laigneville, 60290, France*

[4] *Université du Québec à Chicoutimi, Department of Applied Sciences, 555, boul. de l'Université, Saguenay, Québec, Canada, G7H 2B1*

(Corresponding author / E-mail address: Daniel.Larouche@gmn.ulaval.ca)*
(Tel.:1-418-656-2153; Fax: 1-418-656-5343)

ABSTRACT

Nowadays, in order to fit environmental restrictions, automotive markets are demanding cast aluminum alloys working at high temperature (180–300°C). New generations of alloys are required for higher strength components in engine downsizing or start-stop systems which lead to higher loading and higher specific power and stretch current materials to their limits. Recently, transition metals, such as zirconium and vanadium, have been added as alloying elements into an AlSi7Cu3.5Mg0.1 alloy to improve physical, mechanical, thermodynamic properties with the aim of increasing service life of parts. In such alloys, the best mechanical properties are associated with the formation of precipitates through an optimum heat treatment sequence, including: solutionizing, quenching and artificial aging. This study is focused on the modified AlSi7Cu3.5Mg0.1 cast alloy with Mn, Zr and V additions for high temperature application. The characterization of the cast alloy in this study, firstly, helps to evaluate and understand its performance both chemically and structurally according to their physical state: as-cast or as-quenched. Comparison of precipitation kinetics between a binary Al-3.5%wt.Cu alloy and the AlSi7Cu3.5Mg0.1 (Mn, Zr, V) alloy has been characterized by differential scanning calorimetry, TEM observations and micro-hardness testing. The Kissinger analysis was applied to extract activation energies from non-isothermal DSC runs conducted at different stationary heating rates. The study focuses on the impact of the chemical composition such as Si content on the kinetics parameters.

KEYWORDS

AlSi7Cu3.5Mg0.1 alloy, Al-Cu alloys, Differential Scanning Calorimetry (DSC), Precipitation kinetics

INTRODUCTION

Pure metal Aluminum shows poor mechanical properties and its malleability is high, that is why alloying elements are added to the mixture before casting to improve physical, mechanical and thermodynamic properties (Javidani, 2015); such as Silicon (Si) for casting properties (castability, cold crack capability, wear resistance, shrinkage behavior), Magnesium (Mg) and Copper (Cu) to generate precipitation hardening systems. Aluminum hypoeutectic alloys (<12% Silicon) with Cu, Mg additions used in the automotive industry for manufacturing mechanical parts (Larouche & Javidani, 2014) are mostly subject, after casting, to precipitation hardening heat treatment (Mohamed & Samuel, 2012) according to specifications and associated standards. The best mechanical properties are associated with the formation of precipitates through an optimum heat treatment sequence, generally including: solutionizing, water quenching and artificial aging (Manente & Timelli, 2011). Hypoeutectic aluminum-copper alloy with amount of Cu around 1 to 4.5wt% is an elementary case for precipitation in heat treatable aluminum alloys. Researchers essentially focused their work on the full precipitation sequence of binary Al-Cu alloy during aging which is presented below.

Supersaturated solid solution → atomic clusters → GPI zones → GPII (θ") → θ' → θ

In recent years, new alloys have been developed in order to upgrade the alloy strength at higher temperatures. Technically, it requires modifying the common composition of aluminum alloys to obtain a microstructure containing thermally stable and coarsened resistant phases. Three criteria are needed. The alloying elements should be able of forming thermally stable intermetallics/strengthening phases, should have low diffusivity and low solubility in the matrix, then, do not impact castability, ductility and fracture toughness. Among the transition metals, V and Zr have low diffusivity and solubility in Al matrix, they form thermally stable complex intermetallics and have been found to maintain their strength at temperatures up to 350°C with precipitation of Al_3Zr, $Al_{21}V_2$ or Al_3(Zr, V, Ti) dispersoids (Elhadari, Patel, Chen, & Kasprzak, 2011; Mahmudi, Sepehrband, & Ghasemi, 2006; Sepehrband, Mahmudi, & Khomamizadeh, 2005; Shaha, Czerwinski, Kasprzak, Friedman, & Chen, 2015). Concretely, today aluminum alloys used for the manufacture of automotive cylinder heads are mainly derived from hypo-eutectic Al-Si family, such as those belonging to the three first main categories presented in Table 1.

Table 1. Hypo-eutectic Al-Si foundry alloys for the manufacture of automotive cylinder heads

	Designations	System	Principal hardening precipitates with precursors
▪	319-type alloy (ASTM)	Al-Si-Cu	Al_2Cu (θ)
▪	356-type alloy (ASTM)	Al-Si-Mg	Mg_2Si (β)
▪	356-type +%Cu alloy	Al-Si-Cu-Mg	Al_2Cu (θ), Mg_2Si (β), Q phase or S phase
▪	Very high-temperature alloys	Al-Si-Cu-Mg / Ti-Zr-V	Al-Zr Al-V Al-Zr,V,Ti dispersoids, θ, β, Q or S

In aluminum alloy for precipitation hardening with high Cu content (>1%wt.), kinetics of GP zones and θ' phase formations have received less attention in the literature and it is necessary to know more about the kinetics of precipitation in the temperature range where both phases' formations occur. Depending on the aging temperature and due to the fact that it can also be an autocatalytic precipitation reaction (Starink & Zahra, 1997a), GP zones formation can be really difficult to observe by calorimetric or microhardness measurements and particularly for aging temperature higher than 190°C. Microhardness studies from literature on Al-Cu alloys show a significant increase in hardness value for different aging conditions depending on its isothermal temperature and this increase is explained by the θ' formation.

Recently, the authors studied the precipitation kinetics from non-isothermal DSC kinetic analysis and TEM observations in a binary Al-3.5%wt.Cu alloy. The expected temperature for aging in this study was focused on 190°C because it generates short times of precipitates nucleation (short incubation times) which is easier to characterize and was essentially based on the work of (Starink & Zahra, 1997a) on a kinetic precipitation model applied on similar alloys and their isothermal DSC studies. It was shown that nucleation of θ' phase occurs after 8-10h at 190°C by an exothermic peak in a binary Al-Cu alloy. Therefore, this work was initiated to study and characterize the precipitation kinetics of a binary Al-Cu alloy under water quenching conditions by developing an innovative methodology transposable to any kind

of heat treatable aluminum alloys. Precipitation kinetics was studied by investigating fundamental kinetic parameters on DSC runs from Kissinger methodology including activation energies for formation and growth of precipitates and respective transformed fraction evolutions during isothermal aging. The present study is a direct application of this methodology applied for the AlSi7Cu3.5Mg0.1 (Mn, Zr, V). The fact that solution heat treatment (SHT) substantially affects castings in terms of microstructural and chemical changes in an industrial alloy will be demonstrated with qualitative indexing of observed and measured phenomena particularly on new encountered dispersoids (Zr, V contents). The observations and results about intermetallic phase formation during solidification process was elaborated from numerical approaches by physical and thermodynamic databases in order to validate the identification process according to casting or as-quenched conditions. Then a comparison study will conclude about observed differences on precipitation sequence during aging between both alloys.

KINETIC MODEL

The generic kinetic equation used to model the nucleation and growth of precipitates was firstly proposed by Lee and Kim (Lee & Kim, 1990) and Starink and Zahra (1997b) (LKSZ). According to this equation, the time evolution of the fraction transformed α is given by:

$$\alpha = 1 - \left(1 + c \cdot (k \cdot t)^n\right)^{-\frac{1}{c}} \tag{1}$$

where t is the time and c, k and n are 3 independent kinetic parameters. For the precipitation of a θ phase in a supersaturated matrix, the fraction transformed is given by:

$$\alpha = \frac{g_\theta}{g_\theta^{eq}} \tag{2}$$

where g_θ and g_θ^{eq} are respectively the volume fraction and the equilibrium volume fraction of phase θ at a given temperature. Considering that the nucleation stage is completed at time zero and that the growth of a precipitate is a thermally activated process, the rest of the transformation can be modelled as a single stage reaction process for which k has an Arrhenius type dependency with temperature:

$$k = k_0 \exp\left(-\frac{E}{RT}\right) \tag{3}$$

Kinetic equations describe isothermal transformation; but non-isothermal calorimetric analysis can be used to determine k_0, E for a given $f(\alpha)$ with the variable state concept (Starink, 2013) defined as:

$$\omega = \int_0^{\alpha(t)} \frac{d\alpha}{f(\alpha)} = \int_0^t k_0 \exp\left(-\frac{E}{RT}\right) dt = \int_0^t k dt \tag{4}$$

For a fixed state of transformation ω_f, one can assign a temperature T_f so that (Mittemeijer, 1992):

$$\omega_f = \int_0^{\alpha_f} \frac{d\alpha}{f(\alpha)} \cong k_0 \frac{RT_f^2}{E\dot{T}} \exp\left(-\frac{E}{RT_f}\right) \tag{5}$$

By taking the natural logarithm on both sides of Eq. (5), one obtains:

$$R \cdot \ln\left[\frac{T_f^2}{\dot{T}}\right] = \frac{E}{T_f} - R \cdot \ln\left(\frac{R}{E}\frac{k_0}{\omega_f}\right) \tag{6}$$

The temperature at the top of a DSC peak can therefore be considered as the maximum rate of conversion. It corresponds to $\omega_f = \omega_{peak}=1$ for $T_f = T_{peak}$. Examination of Eq. (6) reveals that the activation energy E can easily be determined from the slope of the curve obtained by plotting $R\cdot\ln\left(T_{peak}^2/\dot{T}\right)$ against $1/T_{peak}$. The pre-exponential factor k_0 is evaluated from the intercept value occurring between the previous curve and the vertical axis. The value of k in the LKSZ at different temperatures can then be well evaluated by this method. One can estimate the impingement factor (c), by fitting the impact of the LKSZ equation on the experimental DSC curve dα/dt, the latter being determined from (Chen, Mussert, & van der Zwaag, 1998):

$$\frac{d\alpha}{dt}=\frac{1}{\Delta h}(q-q_B) \tag{7}$$

where q is the power measured by the DSC, q_B is the baseline and Δh is the total latent heat released during the reaction. Fitting can be optimized using non-linear method of minimization of least squares error.

EXPERIMENTAL

Sample Preparation

Ingots of AlSi7Cu3.5Mg0.1 (Mn, Zr, V) alloy were elaborated by Rio Tinto and cylindrical samples (ø21 mm, 200 mm length) were cast in the R&D center of Montupet (Laigneville, France). The samples were produced with the gravity die casting technique using a thermo-regulated metallic mold according to NF A57-702-1981 AFNOR standard with Sr modification beforehand. The chemical composition was determined with the instrument ICP-AES - IRIS Intrepid of Thermo Scientific and is given in Table 2. A cast checking and quality monitoring was performed for the production. Casting conditions were optimized (mold and metal temperatures) in order to obtain a Secondary Dendrite Arm Spacing (SDAS) between 15 and 25 µm (17.6 µm ±3.2 µm measured), representative of those observed in cylinder fire deck surface (Lombardi, D'Elia, Ravindran, & MacKay, 2014). Samples were thus cast under the following conditions, 709°C ±6°C in the ladle at the time of casting in the die at 149°C ±6°C. The solution heat treatment of the AlSi7Cu3.5Mg0.1 (Mn, Zr, V) alloy was done at 505°C during 4 h with an initial slow heating of 1h 15 and followed by cold water quenching. The binary Al-3.5%wt.Cu alloy was prepared by mixing pure aluminum and controlled amount of pure copper. Sampling from the melt was carried out with Pyrex tubes equipped with a propipette. Tubes with a 5 mm inside diameter and 2 mm wall thickness were used for this purpose. The temperature of the solution heat treatment, after a slow heating (1h 15) was 500°C; a second step of SHT was applied at higher temperatures at 550°C both for 8 h. After the 18 h SHT, the specimens were quenched into cold water to obtain the maximum solute saturation.

Table 2. General chemical composition of cast alloy from cast ingots

AlSi7Cu3.5Mg0.1 (Mn, Zr, V)	**Elements**	**Si**	**Cu**	**Mg**	**Fe**	**Ti**	**Sr**	**Mn**	**Zn**	**P**	**Zr**	**V**
	% wt.	7	3.5	0.1	0.1	0.1	0.015	0.15	0.005	0.005	0.1	0.1

Characterization Methods

AlSi7Cu3.5Mg0.1 (Mn, Zr, V) Characterization in As-Cast Condition

Samples for microstructural examination were sectioned from the cast cylinder, mounted, ground, and polished using standard procedure. The polished sections were then examined with an optical microscope and with electron probe microanalysis (EPMA-CAMECA SX100 with W filament) equipped with a wavelength dispersive spectrometer (WDS). SEM observations have been done on a FEI QUANTA-250 assisted by a microanalyzer X EDS and a gold-palladium metallization device for conductive layer deposition (10–20 nm thickness). EPMA and SEM used energies were respectively 15 and 30 keV.

Power Compensation Differential Scanning Calorimetry of Quenched Specimens

Small samples of 4.5 mm diameter and having a thickness of ≈ 2 mm were prepared for DSC analysis from the quenched cylinders. The specimens were held for few hours at room temperature before

their heating in the DSC device in order to limit the effects of natural aging. Samples have been characterized by non-isothermal DSC analysis with the PerkinElmer Diamond instrument. The latter was calibrated for one heating rate (12.5°C/min). Measurements were conducted with all samples and references prepared with the exact same mass (±0.01mg). The instrumental baselines were performed with pure aluminum in the sample and reference furnaces for each heating rates. Constant heating rates of 1, 2, 4, 6, and 8 K/min were applied and two different samples were analyzed for each heating rate for reproducibility. Generic binary Al-3.5%wt.Cu alloy peaks identification was developed with literature comparison (Choi, Cho, & Kumai, 2016; Elgallad, Zhang, & Chen, 2017; Fatmi et al., 2013; Fu et al., 2014; Hayoune & Hamana, 2009; Ovono Ovono, Guillot, & Massinon, 2007; Son, Takeda, Mitome, Bando, & Endo, 2005; Starink & Van Mourik, 1992) for similar alloys and with temperature expectations from available metastable phase diagram.

Microhardness, TEM Preparation and Observations

Isothermal runs on selected samples were interrupted at 190°C in order to subject them to Vickers microhardness tests at room temperature. Microhardness experiments were conducted on Clemex CMT using a load of 0.0098 N with a dwell time of 13 s. To ascertain reproducibility and statistical validity, 10-16 microhardness tests were performed at each condition. Only intradentritic measurements were performed. Vickers microhardness indentations showing difference in the lengths of the diagonals over 5% of the mean were discarded. The typical accuracy as calculated from the standard deviation in a set of hardness data according to the number of indentations was about ±3 HV. Disks and pieces were cut from quenched cylinders and get heat treated and aged at different conditions. TEM samples have been prepared by electro-polishing from previous heat treated samples. Precipitates observations by transmission electron microscopy on Al matrix plans for the different aging conditions have been done with a Jeol JEM-2100F TEM on 2F-1g or 2g matrix condition in g200 of aluminum near [001] axis and also in g200 near [011] axis.

RESULTS

As-Cast and As-Quenched Metallurgical Characterization

Cast AlSi7Cu3.5Mg0.1 (Mn, Zr, V) samples have millimetric grain size and measured SDAS of 17.6 µm ±3.2 µm. The as-cast microstructures show very low porosity but many types of intermetallics (Figure 1). Microanalysis X EDS has been done inside a dendrite in order to estimate which elements are present in the Al matrix and the results show that Al, Si, Cu and Zr were the major elements in the FCC matrix. The intermetallics are identified in Figure 1 based on literature (Samuel, Samuel, Doty, Valtierra, & Samuel, 2013), thermodynamic computations and the as-cast microprobe cartography analysis. It can be seen that the fibrous silicon eutectic constituent is surrounded by Cu, Mn, Fe, Mg and Si content intermetallics.

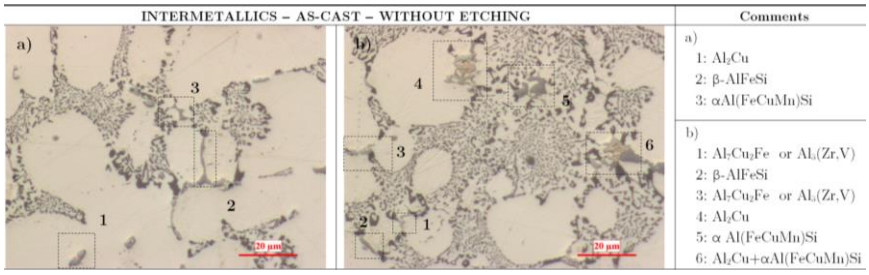

Figure 1. As-cast intermetallics met in AlSi7Cu3.5Mg0.1 (Mn, Zr, V) alloy microstructure

Figure 1 show the presence of intermetallic phases like: α-Al(Fe, Cu, Mn)Si, β-AlFeSi, Al_2Cu, Al_7Cu_2Fe, Al_3 (Zr, Ti, V), Al_2Si_2 (Sr). Phase formation was simulated in this study to estimate numerically the mass fractions of solid phases formed during solidification via the Scheil module of Thermo-Calc

software using TTAL7 database. The evolution of mass fraction of the potential phases has been calculated and was in accordance with those observed in the micrographies.

From the as-cast condition, a solutionizing heat treatment was conducted with an average heating rate of 8.5°C/min to 505°C, followed by a holding period of 4 h. Figure 2 combines the impact of the solutionizing + quenching on the microstructure of the alloy. It is therefore possible to observe firstly the resulting spheroidization of silicon platelets and secondly the dissolution of most of the intermetallics. The residual intermetallics are identified in Figure 2 based on the literature, equilibrium calculation with Thermo-Calc and microprobe cartography analysis. These observations present the general eutectic silicon spheroidization and some undissolved intermetallics containing Cu, Zr or V. The equilibrium calculation performed with Thermo-Calc at 505°C showed that the undissolved phases were α Al(Fe, Cu, Mn)Si, Al_2Si_2 (Sr) intermetallics and remaining Al_3(Zr, V, Ti) dispersoids. The chemical composition in the dendrites was found uniform after the SHT, as this was confirmed by line-scans EPMA.

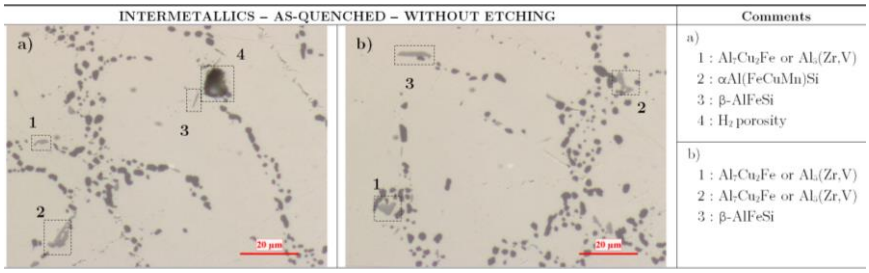

Figure 2. As-quenched intermetallics met in AlSi7Cu3.5Mg0.1 (Mn, Zr, V) alloy microstructure

DSC Runs for Constant Heating Rate

The non-isothermal methodology developed permits to obtain precipitation peaks for different constant heating rates as shown in Figure 3 for the AlSi7Cu3.5Mg0.1 (Mn, Zr, V) alloy. Three peaks A, B, C have only been analyzed. In the previous study on the binary Al-3.5%wt.Cu alloy, three similar precipitation peaks were obtained. Based on the literature and MatCalc predictions, the peaks were associated to the formation of GP zones, θ' and θ respectively in the kinetic sequence of precipitation

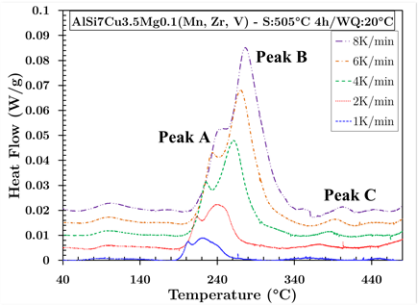

Figure 3. DSC runs for 1-2-4-6-8 K/min heating rates for as-quenched AlSi7Cu3.5Mg0.1 (Mn, Zr, V) alloy

Determination of Kinetic Parameters by the Kissinger Method

As described in previous section, the Kissinger method was applied to analyze the precipitation kinetics of the alloy. Table 3 summarizes the measured peak temperatures obtained at different heating rates. The Kissinger diagram obtained is presented in Figure 4. The non-symmetric aspect of the peak is caused by successive growth and dissolution processes which generate some complexity and uncertainty in the analysis. Activation energies E and the values for k_0 are presented in Table 4. The parameters c and Δh were evaluated from graphical fitting with the DSC curves.

Table 3. PC-DSC peak temperatures T_f=T_{Peak} obtained at different heating rates $\dot{T}$ for the studied alloy

Heating rate (K/min)	*Peak A*		*Peak B*		*Peak C*	
1	206.3	204.6	223.2	221.3	353.3	355.3
2	217.9	214.6	243.2	239.3	372.1	373.3
4	225.9	226.0	262.5	261.3	384.8	385.6
6	234.5	234.5	270.8	269.8	391.6	393.3
8	247.5	244.5	276.2	276.7	401.1	403.5

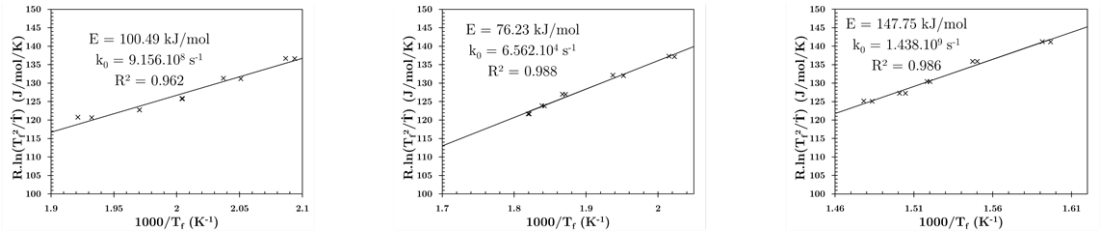

a) *b)* *c)*

Figure 4. Kissinger diagrams for AlSi7Cu3.5Mg0.1 (Mn, Zr, V) alloy: a) Peak, b) Peak B, c) Peak C

Table 4. Parameters from the fitting procedure for AlSi7Cu3.5Mg0.1 (Mn, Zr, V) alloy

Precipitate	*E (kJ/mol)*	*k_0 (s^{-1})*	*n*	*c*	*Δh (mJ)*
Peak A	100.49	$9.156.10^7$	3	1	450
Peak B	76.22	$6.562.10^4$	3	1.7	2200
Peak C	147.75	$1.438.10^9$	3	4	60

Figure 5a presents the obtained fitting parameters for a 6 K/min heating rate analysis. The fitting is not perfect due to the dissolution process of each coherent/semi-coherent phases which have not been simulated. The isothermal evolutions of fraction transformed at 190°C and 350°C of each precipitate calculated with the LKSZ kinetic equation are presented respectively in Figures 5b and 5c. In the binary Al-3.5%wt.Cu alloy, at 190°C, GP zones and θ' started to nucleate after 0.2 h and 3 h, respectively. At 350°C, GP zones and θ' formed almost instantaneously but θ formation begins after 10 h. In AlSi7Cu3.5Mg0.1 (Mn, Zr, V) alloy, it takes less than 1 h for peak A et B to begin at 190°C and at 350°C, peak A and B appears instantaneously and peak C is observed since the beginning of aging. Microhardness measurements on both alloys for different aging time at 190°C show changes in phase formation. For binary Al-3.5%wt.Cu alloy, it happens between 6 and 10 h and between 0.5 and 2 h for AlSi7Cu3.5Mg0.1 (Mn, Zr, V) alloy due to a significant increase in microhardness value. Similar results for the latter can be compared in work of Mahmudi et al. (2006), Ibrahim, Samuel, Samuel, Al-Ahmari, and Samuel (2011), Tavita-Medrano (2007) or Ovono Ovono (2004).

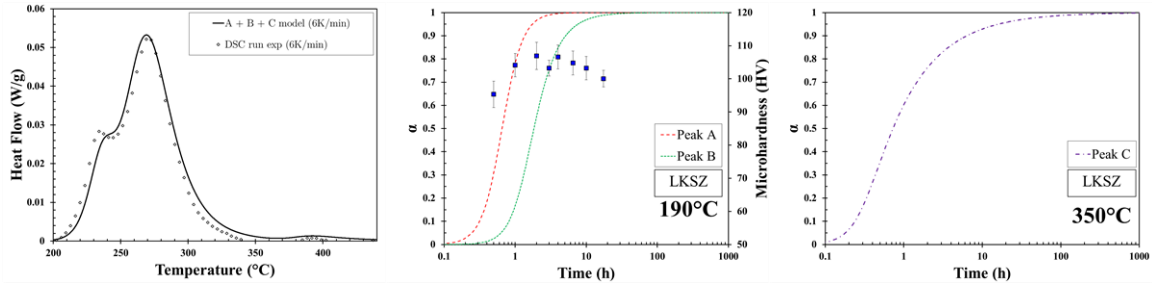

a) *b)* *c)*

Figure 5. a) DSC run and peaks (A, B, C) adjusted to optimize the fit between experimental and sum of the heat produced by associated transformations for AlSi7Cu3.5Mg0.1 (Mn, Zr, V) alloy; Isothermal evolution of the fraction transformed α as calculated by the LKSZ kinetic model, a) at 190°C associated with microhardness results during aging, b) at 350°C

TEM Precipitate Observations

Isothermal aging at 190°C have been studied with two time conditions: 6 h and 12 h for binary Al-3.5%wt.Cu alloy. Associated TEM observations near [001] axis in g200 to beam conditions are presented in Figures 6a and 6b. Semi-coherent θ' metastable phase has globally been characterized in both conditions. Indeed, this observation is validated by dark field images. In some regions, very few small coherent θ stable precipitates (≤ 250 nm in length) are present as reported by EDS analysis and high resolution Selected Area Electron Diffraction (SAED) identification. After aging at 350°C during 1h in binary Al-3.5%wt.Cu, huge θ' precipitates were formed as one can see on Figure 6c. These precipitates have diameters larger than 500 nm. For the AlSi7Cu3.5Mg0.1 (Mn, Zr, V) alloy, similar isothermal aging conditions have been tested. TEM observations near [011] axis in g200 to beam conditions are presented in Figure 7. After aging at 190°C, two major kinds of precipitates can be observed. Thin perpendicular ones are referred as θ' metastable phase and little dark rounded ones as Al_3(Zr, V, Ti) dispersoids from EDS results. During aging at 350°C, also two major kinds of precipitates can be identified. Both precipitates are incoherent with Al matrix and are possibly associated with θ stable phase (grey little dispersoids) and Si precipitates (globular dark ones) which have been likely retarded by the presence of strontium and can be obtained only for higher aging temperatures as explained in (Hernandez Paz, 2003). This preliminary identification from EDS analysis remains to be conducted with SAED patterns results on high magnification precipitates.

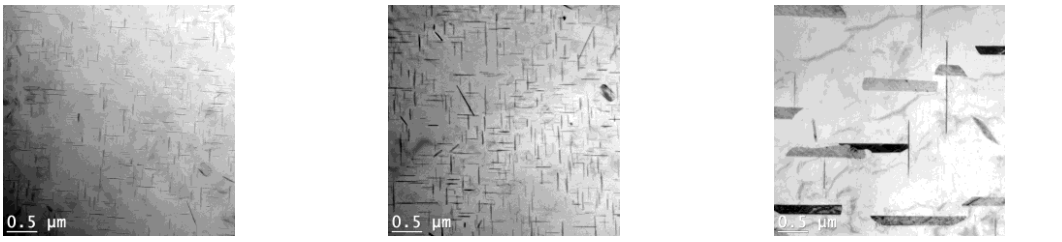

a) aged 6 h at 190°C along axis <001> *b) aged 12 h at 190°C along axis <001>* *c) aged 1 h at 350°C along axis <011>*

Figure 6. TEM observations for binary Al-3.5%wt.Cu alloy in g200 to beam conditions

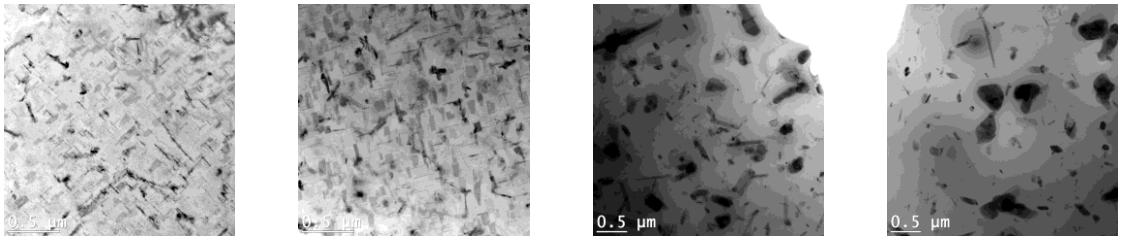

a) aged 30min at 190°C *b) aged 6h at 190°C* *c) aged 1h at 350°C* *d) aged 12h at 350°C*

Figure 7. TEM observations for AlSi7Cu3.5Mg0.1 (Mn, Zr, V) alloy along axis <011> in g200 to beam conditions

DISCUSSION

Metallurgical Characterization of AlSi7Cu3.5Mg0.1 (Mn, Zr, V)

Microhardness results provide a good demonstration of phase transformation according to the applied aging conditions for time and temperature. Due to the fact that all measurements have been done inside the dendrite, it appears clearly that its evolution is defined by a nanoscale hardening. According to related publications from the literature, an increase in measured microhardness can be ascribed to the formation of a metastable phase. It clearly appears that the precipitation of metastable phases in AlSi7Cu3.5Mg0.1 (Mn, Zr, V) alloy occurs rapidly at 190°C, while this occurs after some hours in a binary Al-Cu alloy (Silcock, Heal, & Hardy, 1954).

Calorimetric Precipitation Study

The parameters determined by the Kissinger analysis are very important as they help to provide fraction transformed as a function of time during an isothermal aging. Different values of the activation energies are reported in the literature for θ' (Barlas, 2004; Ovono Ovono et al., 2007; Smith, 1998) and θ (Barlas, 2004). In the binary Al-Cu alloy, the activation energy associated to the precipitation kinetics of θ is approximately 3 times the value obtained for θ' according to respective growth processes. In the AlSi7Cu3.5Mg0.1 (Mn, Zr, V) alloy, if we consider that peak A and B are referred as GP Zones and θ' precipitates formations respectively, activation energies associated to the precipitation kinetics of GP Zones (peak A) is 100 kJ/mol and the value obtained for θ'(peak B) is 76 kJ/mol. Those two values are smaller by about 40 kJ/mol compared to binary Al-Cu alloy. If the peak C in the AlSi7Cu3.5Mg0.1 (Mn, Zr, V) alloy is assimilated to the formation of θ, the activation energy of this stable phase (148 kJ/mol) is less than half the value obtained for θ in a binary Al-Cu alloy (330 kJ/mol). But it appears that the activation energy for peak C is in agreement with those from one study in similar alloy (Barlas, 2004). Evolutions of transformed fraction in isothermal analysis from Figure 5b are in agreement with microhardness measurements evolutions during aging at 190°C. As for the results for the generic binary Al-Cu alloy with (Starink & Zahra, 1997a), those observations are in adequacy with literature in (Mahmudi et al., 2006), (Ibrahim et al., 2011), (Tavita-Medrano, 2007) or (Ovono Ovono, 2004) for Al-Si-Cu alloys. Figure 5c presents evolution of transformed fraction for peak C in studied AlSi7Cu3.5Mg0.1 (Mn, Zr, V) alloy during aging at 350°C. Considering the assumption that peak C in the latter corresponds to θ formation, it appears that it occurs extremely faster in AlSi7Cu3.5 alloy than in binary Al-Cu alloy and possibly due to differences in Si content. Isothermal analysis from Kissinger methodology appears to be an interesting way to estimate nucleation time (or incubation time) for different precipitates in heat treatable aluminum alloys. Next improvements could be considered by taking into account dissolution processes in the precipitation sequence with associated and accurate peaks deconvolution.

Nanoscale Precipitate Observations by TEM

Studied conditions in TEM observations are presented in Figures 6 and 7 for binary Al-3.5%wt.Cu and AlSi7Cu3.5Mg0.1 (Mn, Zr, V) alloys, respectively. In the generic binary alloy, Figures 6a and 6b provide an overview of the growing process of θ' precipitates. It is important to notice local presence of some incoherent θ precipitates (almost 20 times less in density than θ') which has been characterized by SAED and EDS analysis. In the AlSi7Cu3.5Mg0.1 (Mn, Zr, V) alloy, Figures 7a and 7b present samples aged at 190°C during 30 min and 6 h. EDS analysis on selected precipitates permits to approach a first identification of them. Those are supposed to be θ' metastable phase and Al_3(Zr, V, Ti) dispersoids. Figure 6c shows huge θ' precipitates in binary Al-3.5%wt.Cu alloy after an aging at 350°C during 1h. This picture can be compared with Figure 7c for AlSi7Cu3.5Mg0.1 (Mn, Zr, V) alloy in similar conditions where only θ and Si precipitates can be observed. These differences can be explained by evolutions of transformed fraction in isothermal analysis in Figure 5c. Indeed, considering the assumption that peak C in AlSi7Cu3.5Mg0.1 (Mn, Zr, V) alloy corresponds to θ formation and growth, the latter is expected to start sooner than in a binary Al-Cu alloy which is verified by TEM observations. Respective comparisons between Figures 7a and 7b and Figures 7c and 7d present a widespread growth of observed precipitates.

CONCLUSIONS

As-quenched SEM observations in AlSi7Cu3.5Mg0.1 (Mn, Zr, V) alloy confirm that rich copper and magnesium intermetallics almost totally dissolve in the FCC matrix during SHT by diffusion. Although diffusion can improve homogenization process, iron, manganese, zirconium and vanadium intermetallics still remain undissolved in the alloy after SHT due to their very low diffusion coefficient. Solid phase transformation occurrences have been confirmed with TEM observations and microhardness testing from isothermal aging conditions. Precipitation sequences in both alloys have been investigated and results may be summarized as follows:

- DSC curves of AlSi7Cu3.5Mg0.1 (Mn, Zr, V) alloy present three major exothermic events (peaks A to C). Assumption on peaks identification according to preliminary results from EDS spectrums has been made. Peaks A, B and C may similarly correspond to GP zones, θ' and θ formations.

- Obtained activation energies for θ’ and θ formation are similar to data from literature according to their respective chemical composition. The activation energies for θ’ and θ formation are in the range of 76 and 148 kJ per mol respectively for the AlSi7Cu3.5Mg0.1 (Mn, Zr, V), which are significantly less than those found by many authors for binary Al-Cu alloys.
- Isothermal calorimetry data from kinetic study was analyzed and compared with experimental TEM observations and correspond well with literature data for different aging conditions.
- Si content seems to have a large impact on stability of precipitates. Indeed, high Si content in a casting alloy will help get θ precipitates faster. It also generates short incubation times for θ’ formation.

This study demonstrates that this methodology can be transposed to any aluminum alloys and with any kind of precipitates (θ-Al_2Cu, β-Mg_2Si, S-Al-Cu-Mg, Q-Al-Si-Cu-Mg) as observed in hypo-eutectic Al-Si cast aluminum alloys for automotive applications.

ACKNOWLEDGMENTS

The authors would like to thank the Natural Sciences and Engineering Research Council of Canada (NSERC) for financial support. The authors are also grateful to J.-P. Masse from (CM)² at École Polytechnique of Montreal for his strong collaboration in conducting the TEM observations.

REFERENCES

Barlas, B. (2004). *Etude du comportement et de l'endommagement en fatigue d'alliages d'aluminium de fonderie.* (PhD thesis), Ecole Nationale Supérieure des Mines de Paris, France.

Chen, S. P., Mussert, K. M., & van der Zwaag, S. (1998). Precipitation kinetics in Al6061 and in an Al6061-alumina particle composite. *Journal of Materials Science, 33*(18), 4477-4483. doi:10.1023/a:1004414413800

Choi, S. W., Cho, H. S., & Kumai, S. (2016). Effect of the precipitation of secondary phases on the thermal diffusivity and thermal conductivity of Al-4.5Cu alloy. *Journal of Alloys and Compounds, 688*, 897-902. doi:10.1016/j.jallcom.2016.07.137

Elgallad, E. M., Zhang, Z., & Chen, X. G. (2017). Effect of quenching rate on precipitation kinetics in AA2219 DC cast alloy. *Physica B: Condensed Matter, 514*, 70-77. doi:10.1016/j.physb.2017.03.039

Elhadari, H. A., Patel, H. A., Chen, D. L., & Kasprzak, W. (2011). Tensile and fatigue properties of a cast aluminum alloy with Ti, Zr and V additions. *Materials Science and Engineering: A, 528*(28), 8128-8138. doi:10.1016/j.msea.2011.07.018

Fatmi, M., Ghebouli, B., Ghebouli, M. A., Chihi, T., Ouakdi, E.-H., & Heiba, Z. A. (2013). Study of Precipitation Kinetics in Al-3.7 wt% Cu Alloy during Non-Isothermal and Isothermal Ageing. *Chinese Journal of Physics, 51*(5), 1019-1032. doi:10.6122/CJP.51.1019

Fu, S., Yi, D.-q., Liu, H.-q., Jiang, Y., Wang, B., & Hu, Z. (2014). Effects of external stress aging on morphology and precipitation behavior of θ″ phase in Al-Cu alloy. *Transactions of Nonferrous Metals Society of China, 24*(7), 2282-2288. doi:10.1016/s1003-6326(14)63345-8

Hayoune, A., & Hamana, D. (2009). Structural evolution during non-isothermal ageing of a dilute Al–Cu alloy by dilatometric analysis. *Journal of Alloys and Compounds, 474*(1-2), 118-123. doi:10.1016/j.jallcom.2008.06.070

Hernandez Paz, J. F. (2003). *Heat Treatment and Precipitation in A356 Aluminum Alloy.* (PhD thesis), McGill University, Montreal.

Ibrahim, M. F., Samuel, E., Samuel, A. M., Al-Ahmari, A. M. A., & Samuel, F. H. (2011). Metallurgical parameters controlling the microstructure and hardness of Al–Si–Cu–Mg base alloys. *Materials & Design, 32*(4), 2130-2142. doi:10.1016/j.matdes.2010.11.040

Javidani, M. (2015). *Effect of Cu, Mg and Fe on solidification processing and microstructure evolution of Al-7Si based foundry alloys.* (PhD), Université Laval, Québec.

Larouche, D., & Javidani, M. (2014). Application of Cast Al-Si Alloys in Internal Combustion Engine Components. *International Materials Reviews, 59*((3)), 132-158.

Lee, E. S., & Kim, Y. G. (1990). A transformation kinetic model and its application to Cu-Zn-Al shape memory alloys-I. Isothermal conditions. *Acta Metallurgica Et Materialia, 38*(9), 1669-1676. doi:10.1016/0956-7151(90)90009-6

Lombardi, A., D'Elia, F., Ravindran, C., & MacKay, R. (2014). Replication of engine block cylinder bridge microstructure and mechanical properties with lab scale 319 Al alloy billet castings. *Materials Characterization, 87*, 125-137. doi:10.1016/j.matchar.2013.11.006

Mahmudi, R., Sepehrband, P., & Ghasemi, H. M. (2006). Improved properties of A319 aluminum casting alloy modified with Zr. *Materials Letters, 60*(21-22), 2606-2610. doi:10.1016/j.matlet.2006.01.046

Manente, A., & Timelli, G. (2011). Optimizing the heat treatment process of cast aluminium alloys *Recent Trends in Processing and Degradation of Aluminium Alloys* (Edited by Prof. Zaki Ahmad ed., pp. 197-220): www.intechopen.com.

Mittemeijer, E. J. (1992). Review, Analysis of the kinetics of phase transformations *Journal of materials Science, 27*, 3977-3987.

Mohamed, A. M. A., & Samuel, F. H. (2012). A review on the heat treatment of Al-Si-Cu-Mg casting alloys. In F. Czerwinski (Ed.), *Heat Treatment – Conventional and Novel Applications*: InTech.

Ovono Ovono, D. (2004). *Recyclabilité des alliages d'aluminium de fonderie : influence des éléments résiduels sur la microstructure et le comportement mécanique.* (PhD thesis), Université de Technologie de Compiègne, France.

Ovono Ovono, D., Guillot, I., & Massinon, D. (2007). Determination of the activation energy in a cast aluminium alloy by TEM and DSC. *Journal of Alloys and Compounds, 432*(1-2), 241-246. doi:10.1016/j.jallcom.2006.05.132

Samuel, E., Samuel, A. M., Doty, H. W., Valtierra, S., & Samuel, F. H. (2013). Intermetallic phases in Al–Si based cast alloys: new perspective. *International Journal of Cast Metals Research, 27*(2), 107-114. doi:10.1179/1743133613y.0000000083

Sepehrband, P., Mahmudi, R., & Khomamizadeh, F. (2005). Effect of Zr addition on the aging behavior of A319 aluminum cast alloy. *Scripta Materialia, 52*(4), 253-257. doi:10.1016/j.scriptamat.2004.10.025

Shaha, S. K., Czerwinski, F., Kasprzak, W., Friedman, J., & Chen, D. L. (2015). Microstructure and mechanical properties of Al–Si cast alloy with additions of Zr–V–Ti. *Materials & Design, 83*, 801-812. doi:10.1016/j.matdes.2015.05.057

Silcock, J. M., Heal, T. J., & Hardy, H. K. (1954). Structural Ageing Characteristics of Aluminum-Copper Alloys. *Journal of the Institute of Metals, 82*, 239-248.

Smith, G. W. (1998). Precipitation kinetics in an air-cooled aluminum alloy: A comparison of scanning and isothermal calorimetry measurement methods. *Thermochimica Acta*(313), 27-36.

Son, S. K., Takeda, M., Mitome, M., Bando, Y., & Endo, T. (2005). Precipitation behavior of an Al–Cu alloy during isothermal aging at low temperatures. *Materials Letters, 59*(6), 629-632. doi:10.1016/j.matlet.2004.10.058

Starink, M. J. (2013). Analysis of aluminium based alloys by calorimetry: quantitative analysis of reactions and reaction kinetics. *International Materials Reviews, 49*(3-4), 191-226. doi:10.1179/095066004225010532

Starink, M. J., & Van Mourik, P. (1992). Cooling and heating rate dependence of precipitation in an Al-Cu alloy. *Materials Science and Engineering A, 156*, 183-194.

Starink, M. J., & Zahra, A.-M. (1997a). Mechanisms of combined GP zone and θ' precipitation in an Al-Cu alloy. *Journal of Materials Science Letters, 16*, 1613-1615.

Starink, M. J., & Zahra, A. M. (1997b). An analysis method for nucleation and growth controlled reactions at constant heating rate. *Thermochimica Acta, 292*(1-2), 159-168. doi:10.1016/s0040-6031(96)03135-8

Tavita-Medrano, F. J. (2007). *Artificial Treatments of 319-Type Aluminum Alloys.* (PhD thesis), McGill University, Montreal.